

Supporting Information

Tailoring Cu⁺ for Ga³⁺ Cation Exchange in Cu_{2-x}S and CuInS₂ Nanocrystals by Controlling the Ga-Precursor Chemistry

Stijn O.M. Hinterding,^{a,§} Anne C. Berends,^{a,†} Mert Kurttepli,^{b,#} Marc-Etienne Moret,^c Johannes D. Meeldijk,^d Sara Bals,^b Ward van der Stam,^{a,‡} and Celso de Mello Donega^{a,}*

^aCondensed Matter and Interfaces, Debye Institute for Nanomaterials Science, Utrecht University, P.O. Box 80000, 3508 TA Utrecht, The Netherlands

^bElectron Microscopy for Materials Science (EMAT), University of Antwerp, Groenenborgerlaan 171, B-2020 Antwerp, Belgium

^cOrganic Chemistry and Catalysis, Debye Institute for Nanomaterials Science, Utrecht University, Universiteitsweg 99, 3584 CG Utrecht, The Netherlands

^dElectron Microscopy Utrecht, Debye Institute for Nanomaterials Science, Utrecht University, 3584 CH Utrecht, The Netherlands

*Corresponding Author: c.demello-donega@uu.nl

Contents

1. Figures referenced from the main text

- Figure S1: TEM sizing histograms of Cu_{2-x}S seed nanocrystals and nanocrystals after Ga^{3+} cation exchange.
- Figure S2: EDS spectrum of $\text{Cu}_{1.03}\text{In}_{0.81}\text{S}_2$ nanocrystals
- Figure S3: Absorption spectra of Cu_{2-x}S seed nanocrystals and nanocrystals after Ga^{3+} cation exchange.
- Figure S4: EDS spectrum of $\text{Cu}_{1.99}\text{Ga}_{0.04}\text{S}$ nanocrystals
- Figure S5: TEM micrograph of Cu_{2-x}S nanocrystals, after reaction with GaCl_3 at 100°C
- Figure S6: HAADF-STEM micrographs and EDS elemental maps of Cu_{2-x}S nanocrystals reacted with GaCl_3 for 120 and 300 min
- Figure S7: EDS spectrum of CGS nanocrystals, after reaction with GaCl_3 -TPP
- Figure S8: EDS spectrum of CGS nanocrystals, after reaction with GaCl_3 -DPP
- Figure S9: TEM micrograph of agglomerated nanocrystals, after reaction with GaCl_3 -DPP
- Figure S10: EDS spectrum of CGS nanocrystals, after reaction with GaCl_3 -DPP under milder reaction conditions

2. Description of calibration of electron-diffraction patterns, with accompanying Figures S11 and S12.

1. Figures referenced from the main text

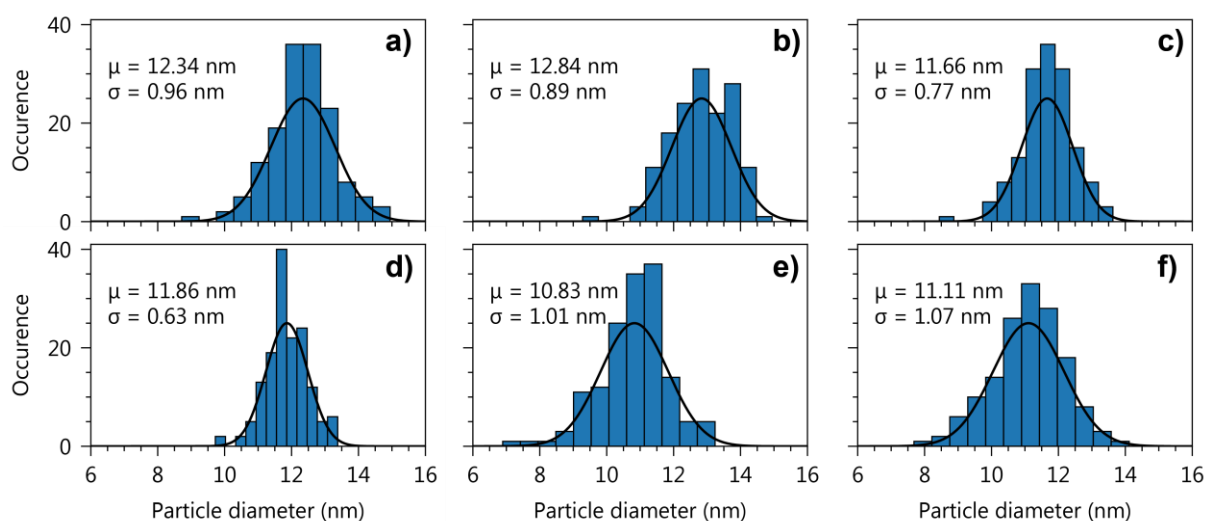


Figure S1. Histograms of particle diameters measured using transmission electron micrographs, of (a) the parent Cu_{2-x}S nanocrystals; and the product nanocrystals obtained after reaction with: (b) $\text{InCl}_3\text{-TOP}$ at 100 °C, (c) $\text{GaCl}_3\text{-TOP}$ at 100 °C, (d) GaCl_3 at 30 °C, (e) $\text{GaCl}_3\text{-TPP}$ at 100 °C and (f) $\text{GaCl}_3\text{-DPP}$ at 100 °C. Black curves represent the corresponding Gaussian distributions, plot using the average (μ) and the standard deviation (σ) of the measured particle diameters. For each sample 150 particles were measured.

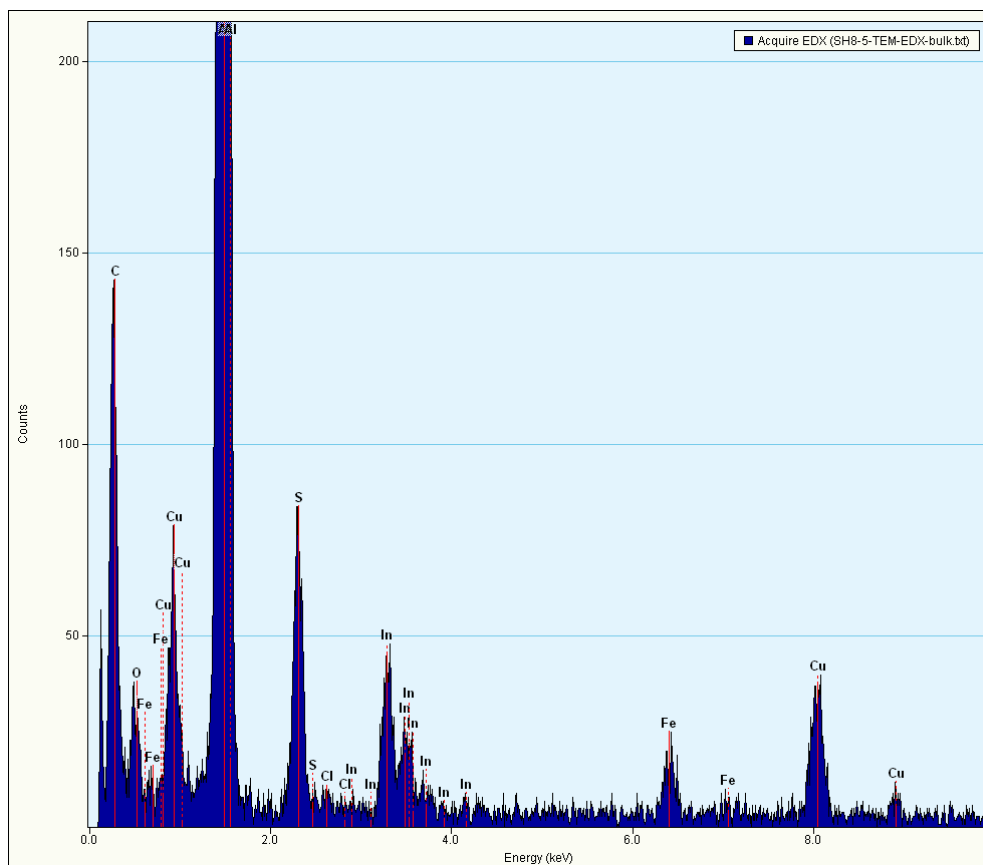


Figure S2. Energy-dispersive X-ray Spectrum (EDS) of $\text{Cu}_{1.03}\text{In}_{0.81}\text{S}_2$ (CIS) bifrustum nanocrystals, obtained after reaction of Cu_{2-x}S nanocrystals with InCl_3 -TOP. Quantification of the spectrum revealed a Cu:In ratio of 1.00:0.79. The spectrum was acquired on a large region containing hundreds of nanocrystals. The aluminium grid used in the measurement causes the peak at around 1.5 keV.

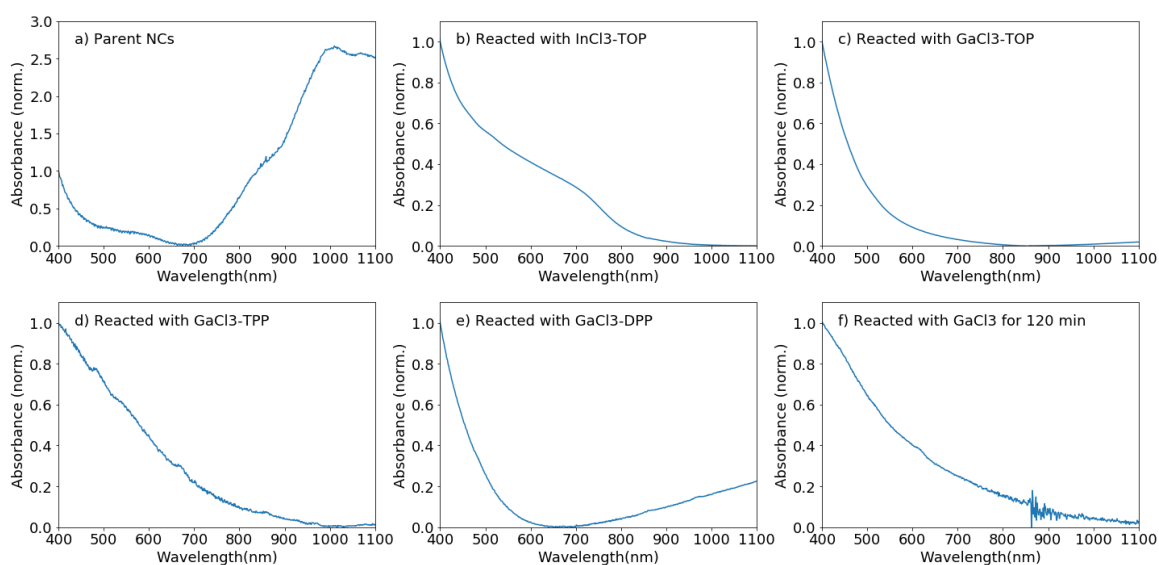


Figure S3. Absorption spectra of (a) the parent Cu_{2-x}S nanocrystals; and the product nanocrystals obtained after reaction with: (b) InCl_3 -TOP at 100 °C, (c) GaCl_3 -TOP at 100 °C, (d) GaCl_3 -TPP at 100 °C, (e) GaCl_3 -DPP at 50 °C and (f) GaCl_3 at 30 °C. Each spectrum was corrected for background absorption, by subtracting a constant background, then normalized to the absorbance at 400 nm.

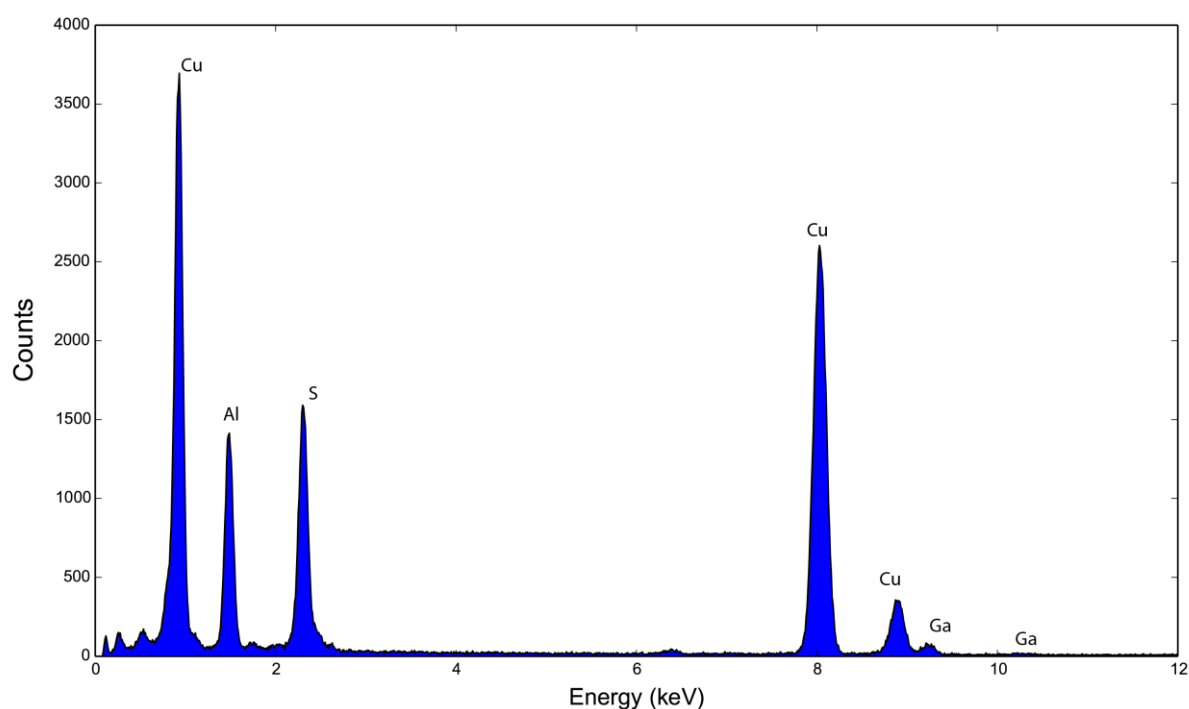


Figure S4. EDS of $\text{Cu}_{1.99}\text{Ga}_{0.04}\text{S}$ nanocrystals, obtained after reaction of Cu_{2-x}S nanocrystals with GaCl_3 -TOP. Quantification of the spectrum revealed a Cu:Ga ratio of 1.00:0.02. The spectrum was acquired on a large region containing hundreds of nanocrystals. The aluminium grid used in the measurement causes the peak at around 1.5 keV.

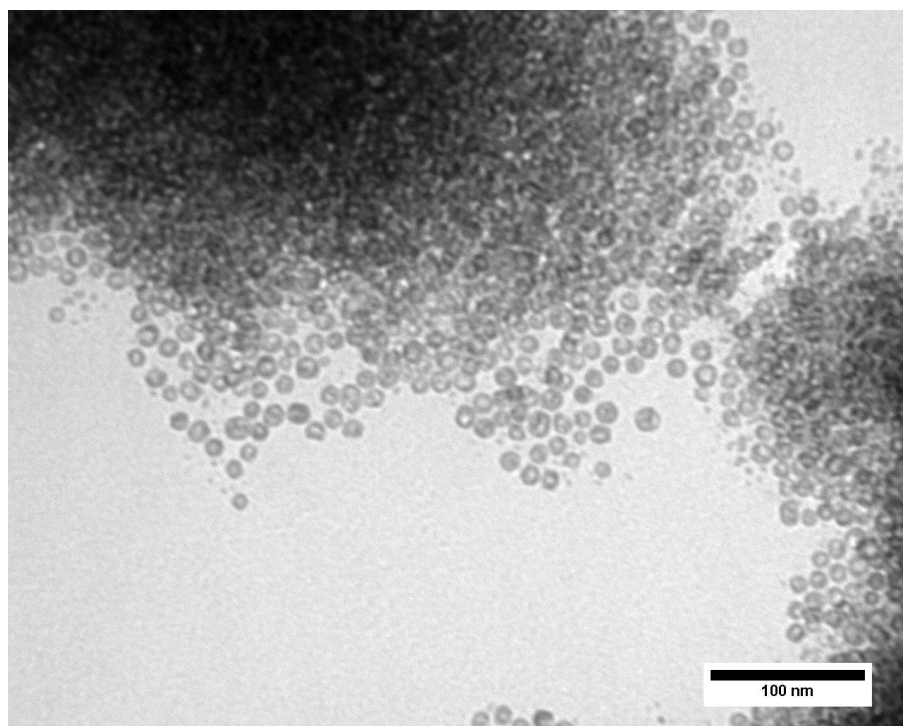


Figure S5. TEM image of Cu_{2-x}S nanocrystals, after reaction with GaCl_3 at 100°C overnight.

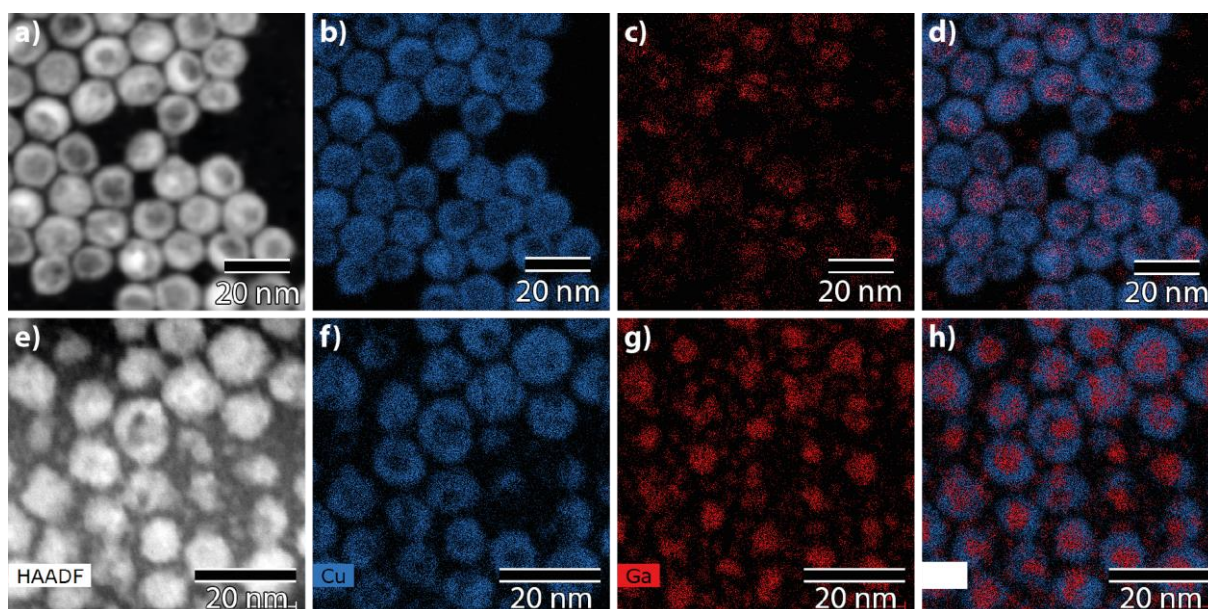


Figure S6. (a) HAADF-STEM micrograph and EDS elemental maps of (b, blue) Cu, (c, red) Ga and (d) Cu and Ga, of Cu_{2-x}S nanocrystals after reaction with GaCl_3 for 120 min. (e) HAADF-STEM micrograph and EDS elemental maps of (f, blue) Cu, (g, red) Ga and (h) Cu and Ga, of Cu_{2-x}S nanocrystals after reaction with GaCl_3 for 300 min.

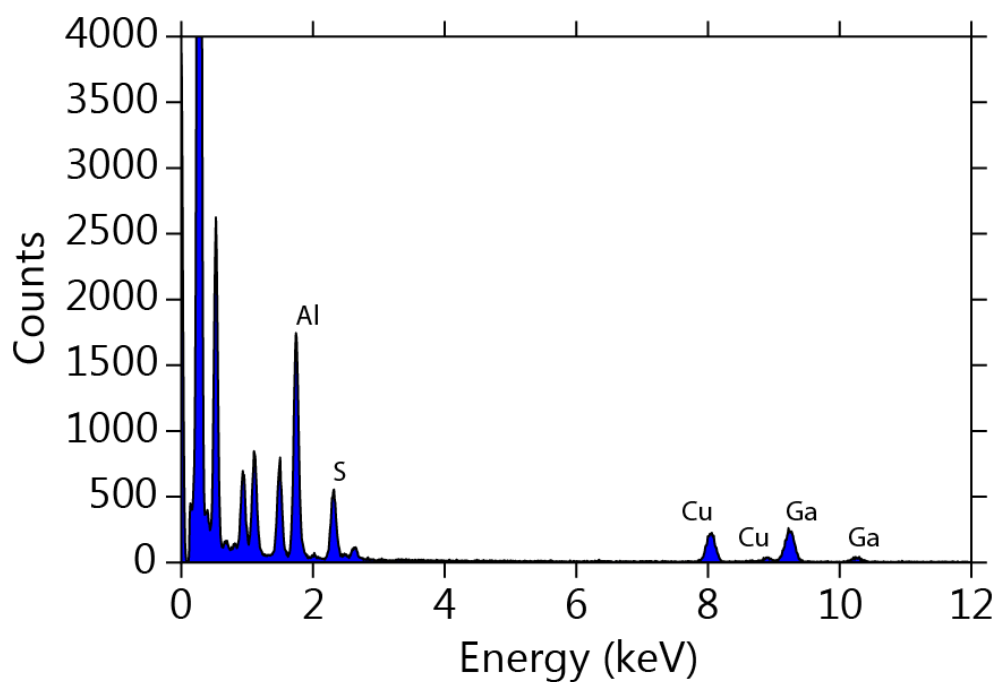


Figure S7. EDS of CGS nanocrystals, obtained after reaction of Cu_{2-x}S nanocrystals with GaCl_3 -TPP. Quantification of the spectrum revealed a Cu:Ga ratio of 1.00:1.38. The spectrum was acquired on a large region containing hundreds of nanocrystals. The aluminium grid used in the measurement causes the peak at around 1.5 keV.

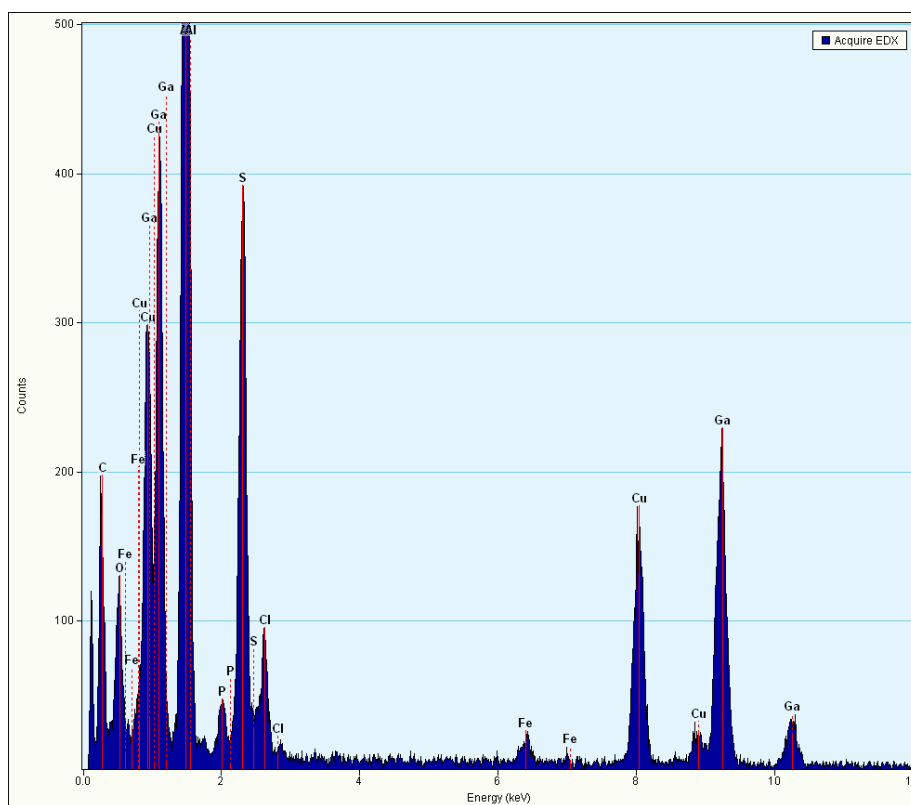


Figure S8. EDS of CGS nanocrystals, obtained after reaction of Cu_{2-x}S nanocrystals with $\text{GaCl}_3\text{-DPP}$. Quantification of the spectrum revealed a Cu:Ga ratio of 1.00:1.48. The spectrum was acquired on a large region containing hundreds of nanocrystals. The aluminium grid used in the measurement causes the peak at around 1.5 keV.

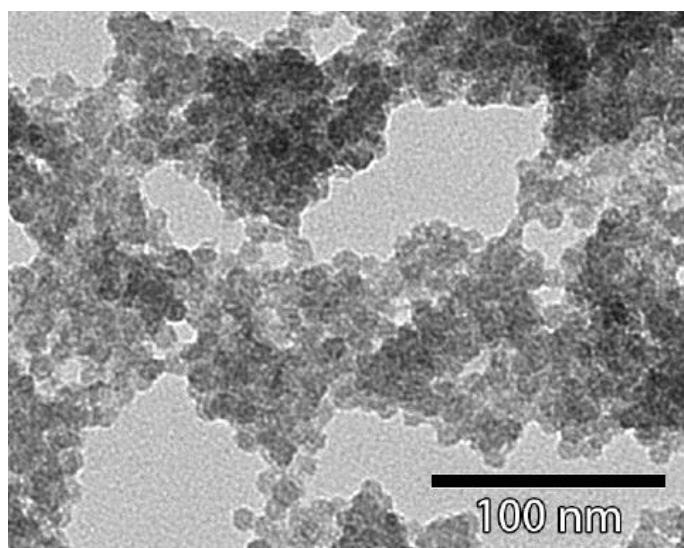


Figure S9. TEM image of agglomerated CGS nanocrystals, obtained after reaction of Cu_{2-x}S nanocrystals with $\text{GaCl}_3\text{-DPP}$.

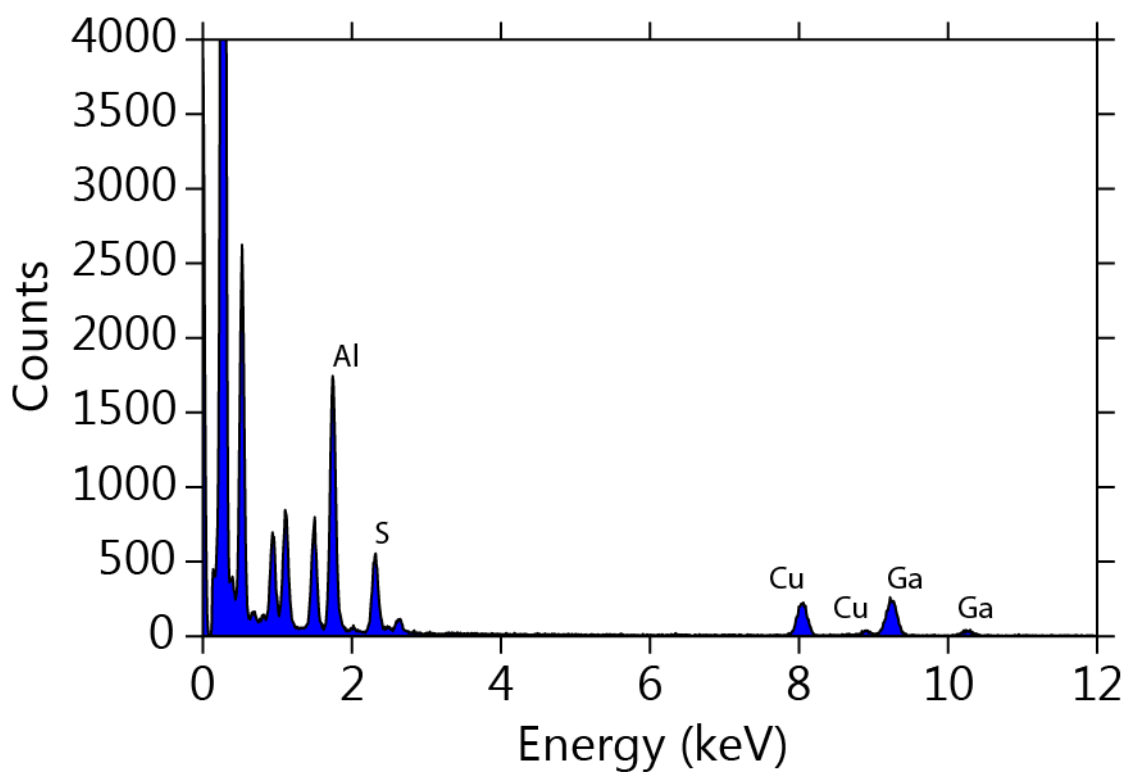


Figure S10. EDS of CGS nanocrystals, obtained after reaction of Cu_{2-x}S nanocrystals with GaCl_3 -DPP under milder reaction conditions (reaction temperature of 50°C) and in the presence of oleylamine ligands. Quantification of the spectrum revealed a Cu:Ga ratio of 1.00:0.62. The spectrum was acquired on a large region containing hundreds of nanocrystals. The aluminium grid used in the measurement causes the peak at around 1.5 keV.

2. Description of calibration of electron-diffraction (ED) patterns

Calibration of the measured ED patterns was performed by measuring the ED pattern of a gold reference sample (Agar S106). The two-dimensional pattern was then reduced to one dimension using the method described in the Experimental section. The known lattice distances of gold in real space, d , were transformed into distances in reciprocal space, q , using the equation $q=2\pi/d$ (Table S1).

Table S1. Lattice planes of cubic close packed gold, with the corresponding real-space lattice spacings d , obtained from JCPDS PDF-card 00-004-0784. The corresponding lattice space in reciprocal space, q , was calculated using $q=2\pi/d$.

Lattice plane	d (Å)	q (nm ⁻¹)
{111}	2.355	26.68
{200}	2.039	30.82
{220}	1.442	43.57
{311}	1.230	51.08

The measured peak maxima (in pixels) were plotted versus q (in nm⁻¹) and fit with a linear equation with an intercept at the origin. The resulting slope (in nm⁻¹pixel⁻¹) was used as calibration constant (or “camera constant”) to convert the horizontal axis of the data from units of pixel into units of nm⁻¹.

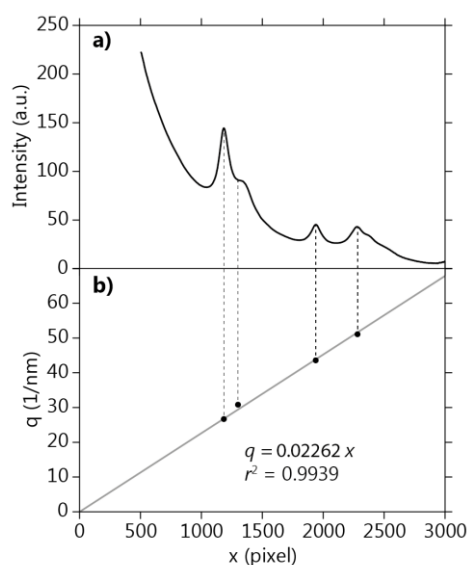


Figure S11. (a) Rotationally averaged electron-diffraction pattern of a gold reference sample and (b) the measured peak maxima plot versus the corresponding reciprocal space lattice spacings q . The resulting data points were fit using a linear equation with an intercept at the origin. The obtained slope was used as calibration constant. Dotted lines serve as guide to the eye.

This calibration procedure was performed for every ED measurement session. Comparison of the peak positions in the ED pattern of CuInS₂ nanocrystals (calculated using the calibration constant) to those in an XRD diffractogram of the same sample shows an excellent agreement (Figure S12), indicating that the ED pattern calibration method used in our work is successful.

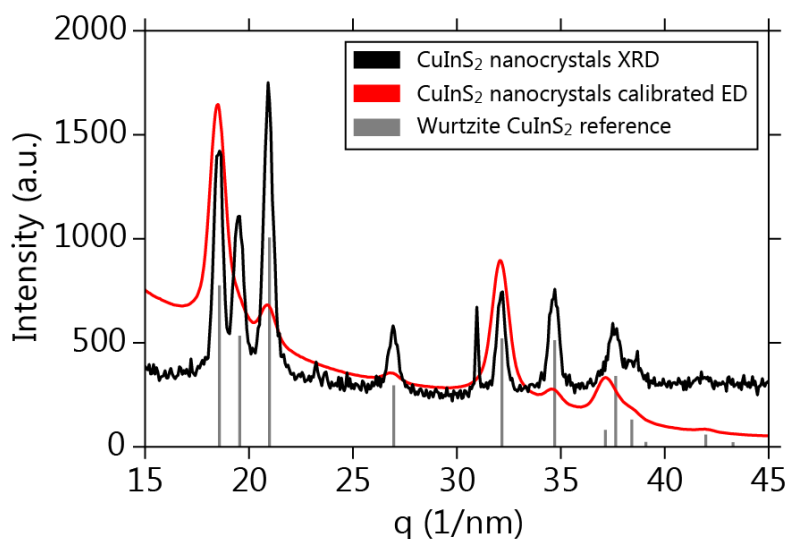


Figure S12. (black) X-ray diffraction (XRD) pattern of CuInS_2 (CIS) nanocrystals, (red) calibrated electron-diffraction pattern of the same sample and (gray) reference bars for the wurtzite CIS crystal structure. The XRD pattern was recorded using a Bruker D2 Phaser, equipped with a $\text{Cu K}\alpha$ X-ray source ($\lambda = 1.54184 \text{ \AA}$). The horizontal axis of the resulting pattern was converted from 2ϑ (units of degrees) into q (units of $1/\text{nm}$) using the equation $q = 4\pi \sin(\vartheta)/\lambda$. Reference bars were obtained from JCPDS PDF-card 01-077-9459.